AD-A185 170 THERMAL STRAIN ANALYSIS USING MOIRE INTERFEROMETRY(U) 1/1
VIRGINIA POLYTECHNIC INST AND STATE UNIV BLACKSBURG
DEPT OF ENGINEERING SCIENCE AND MECHANICS
UNCLASSIFIED P IFJU ET AL. AUG 87 N00014-86-K-0255 F/G 11/4 NL

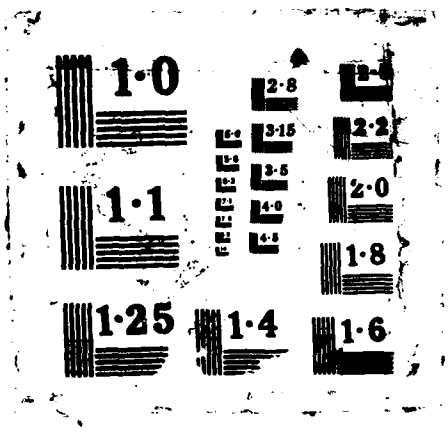
1·0
1·1
1·25
2·8
3·15
3·5
4·0
2·2
2·0
1·8
1·4
1·6

Contract N00014-86-K-0255

SPIE Conf.
August '87

THERMAL STRAIN ANALYSIS USING MOIRE INTERFEROMETRY

P. Ifju, D. Post

Virginia Polytechnic Institute and State University
Department of Engineering Science and Mechanics
Blacksburg, Virginia 24061

ABSTRACT

A method for measuring thermal strains in composites was developed. Strains induced by residual stresses in a cross-ply graphite epoxy specimen were observed. U, V and W displacement fields were revealed using high sensitivity moire and classical interferomery. A specimen grating was replicated on a composite at its stress-free cure temperature (250°F) and deformations were observed at room temperature. The method determines normal strains on a relative basis and shear strains on an absolute basis. A strong free-edge effect was observed; interlaminar shear strains of 1% were recorded near the free edge. Anomalous variations of strains in plies of the same fiber direction were observed throughout the specimen.

1. INTRODUCTION

The thermal coefficients of expansion for each ply of a laminated composite material are smaller in the longitudinal fiber direction and larger in the transverse direction. These composites are cured at elevated temperatures. In the case of a multi-ply laminate with different fiber directions in successive plies, the composite is stress-free at the curing temperature. In cooling to room temperature, however, each ply constrains (decreases or increases) the thermal contraction of its neighbor and residual stresses are developed.

The objective of this study was to reveal the deformations induced by these thermal stresses. A technique was developed to obtain the U and V displacement fields by high sensitivity moire interferometry, and the W field by classical interferometry. The technique is illustrated for a cross-ply composite.

Mechanical mismatch of thermal and mechanical properties also exist between the fiber and matrix materials. Residual strains are developed on the individual fiber scale. These are not studied here, but instead the behavior at the next higher level, the ply level, is investigated. Differences in displacements of neighboring plies are studied.

2. SPECIMEN

The specimen was cut from a thick-walled pressure vessel of graphite-epoxy as illustrated in Fig. 1. Its stacking sequence was $[90_2/0]_{27}$, where the 0 deg fibers were parallel to the axis of the cylinder and the 90 deg fibers were parallel to the hoop direction. The composite was cured at 250°F. After curing, but still at 250°F, the material was assumed to be free of residual stresses.

3. EXPERIMENTAL STUDY

A high frequency diffraction grating was replicated on the specimen at the cure temperature of the composite (250°F). In this case a crossed-line 1200 lines/mm grating was used. Figure 2 illustrates the procedure. Silicone rubber (Sylgard 184 by Dow Corning) was used as the replicating material. First a silicone rubber primer was applied to the face of the specimen. The specimen, and also a holographic grating called a mold, were heated to 250°F in a convection oven. The liquid silicone rubber was then applied between the specimen and mold and squeezed to a thin (≈ 25 μm) film. This operation was done quickly to minimize temperature changes. After 2 hours at 250°F, the silicone rubber had cured. While still at 250°F, the excess silicone rubber around the specimen was cut with a razor and the mold was pried off. This was done at the elevated cure temperature.

The specimen was then cooled to room temperature. Whole-field in-plane displacements were recorded by high-sensitivity moire interferometry [1], using a virtual reference grating of 2400 lines/mm. A four-beam interferometer illustrated if Fig. 3 was used to obtain the U (horizontal) and V (vertical) fields. The basic relationships of moire interferometry are given in the figure. The out-of-plane W displacement field was recorded using a Twyman-Green interferometer [2], illustrated in Fig. 4. The 0 order reflection from the specimen grating comprised the information beam; this interfered with a plane wavefront from the reference mirror to produce a contour map of the specimen surface.

4. FRINGE PATTERNS AND RELATIVE DEFORMATIONS

Fringe patterns of the U, V and W displacement fields are shown in Figs. 5, 6 and 7, respectively. They represent the specimen at a room temperature of 70°F. As the specimen cooled from 250°F, its size and shape changed. The shape changed because of residual stresses that caused stress-induced strains. The size changed because of thermal contractions plus residual-stress-induced strains.

The displacements associated with thermal contraction were not monitored in this work. It is easy to appreciate that the Twyman-Green interferometer pattern gives the topography of the specimen surface at room temperature. Assuming the grating surface was flat at 250°F, this gives the relative W displacement of the surface, i.e., the displacement of any point on the surface relative to the displacement of some reference point on the surface. It does not reveal the absolute change of thickness (z direction) of the specimen.

In a similar way, the U and V fields give relative displacement information. For the room temperature observations, the virtual reference grating frequency was not fixed with respect to the specimen grating frequency at 250°F. Instead, the reference grating frequency was adjusted to produce reasonably sparce patterns at room temperature. The reference datum was arbitrary. As a consequence, unknown gradients ($\partial U/\partial x = C_1$ and $\partial V/\partial y = C_2$) must be added to the U and V patterns to reveal the absolute displacements. What is known, however, is that C_1 and C_2 are constants throughout the field. Consequently, relative deformations are determined by the fringe patterns.

5. RESULTS

Figure 5a shows that the strain ε_x is essentially constant throughout the central region. However, important edge effects occur near the vertical boundaries. The same condition is depicted in Fig. 5b, but with a small change of reference grating frequency to introduce carrier fringes of extension [3]. This enchances the visibility of the edge effect and the extraction of data.

Figure 6a shows that the strain ε_y is different in 0 deg and 90 deg plies. The same condition appears in Fig. 6b, but with carrier fringes that facilitate data extraction. The difference of slopes of fringes in 0 deg and 90 deg plies shows that the ε_y strains differ by 0.4%. This is a representative value, since it is evident from the variation of slopes throughout the pattern that the strain magnitudes do not repeat faithfully on a ply-by-ply basis. The deviations are attributed to variations of material properties in the specimen.

Figure 7a shows the W displacements for a highly-enlarged view near the edge of the specimen. The reference surface was adjusted with a slight inclination with respect to the specimen surface to produce the essentially vertical fringes. The pattern shows that the 90 deg plies contracted less than the 0 deg plies, and protrude 0.3 to 0.5 μm above the 0 deg plies. Again unequal deformations of corresponding plies is evident.

These bulges occur on most of the specimen face, but not at the vertical corners (i.e., at the intersections of vertical faces of the specimen). There, the contraction is constant, independent of ply orientation, and the contraction is smaller than elsewhere on the surface. Figure 7b shows the relative profiles along the centerlines of the plies. This edge effect is confined to a very narrow region near the corners.

A local portion of the U-field is shown in Fig. 8. Shear strains can be calculated on an absolute basis from the U and V fields, using the relationship

$$\gamma_{xy} = \frac{\partial U}{\partial y} + \frac{\partial V}{\partial x} \qquad (1)$$

This is because the unknown parts of the absolute fringe gradients $\partial U/\partial x$ and $\partial V/\partial y$ do not alter the gradients in the perpendicular direction. Consequently, the first cross-derivative in Eq. 1 can be obtained from Fig. 8 and the second from Fig. 6. The result is sketched in Fig. 8 for a representative interlaminar zone between 0 deg and 90 deg plies. It is seen that residual shear strains near the free surface are large, about 1% strain, for the 180°F temperature change. The effect is localized in a narrow zone along the free surface, a zone whose width is equal to 2 to 4 ply thickneses.

This property can be generalized for the present experimental method. While normal strains can be determined only on a relative basis, the shear strains can be determined on an absolute basis.

6. CONCLUSIONS

A practical method was developed to reveal displacement fields induced by residual thermal stresses in a cross-ply composite specimen. High sensitivity moire and classical interferometry revealed the U, V, and W deformations. A specimen grating was applied to the composite at its stress-free cure temperature and its deformation was measured at room temperature. With this method, normal strains are determined as relative values only, while shear strain are determined on an absolute basis. Free edge effects were observed within 2 to 4 ply thicknesses from the edge. Interlaminar shear strains of 1% were measured in this zone for a 180°F change of temperature. Numerical values are representative, since noteable variations occurred throughout the specimen in plies of the same fiber direction.

7. ACKNOWLEDGEMENTS

This work was conducted under sponsorship of the National Center for Composite Materials Research, Urbana, Illinois. The specimen material was provided by the David Taylor Naval Ship Research and Development Center. Special encouragement was given by Dr. Alan Kushner of the Office of Naval Research. The authors are grateful for this generous assistance.

8. REFERENCES

[1] D. Post, "Moire Interferometry", Handbook of Experimental Mechanics, A. S. Kobayashi, Ed., Prentice Hall, Englewood Cliffs, NJ (1987).

[2] F. Jenkins and H. White, Fundamentals of Optics, McGraw-Hill, New York, pp. 253-256 (1957).

[3] Y. Guo, D. Post, and R. Czarnek, "The Magic of Carrier Patterns in Moire Interferometry", International Conference on Photomechanics and Speckle Metrology, August 1987, SPIE Proceedings, Vol. 814, Bellingham, WA.

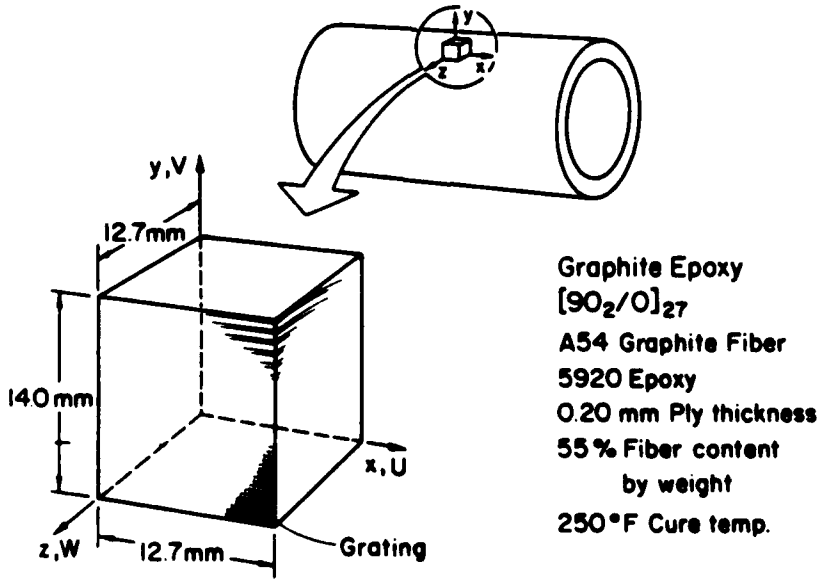

Fig. 1 The specimen was cut from a thick-walled cylinder and a specimen grating was formed on the xy face.

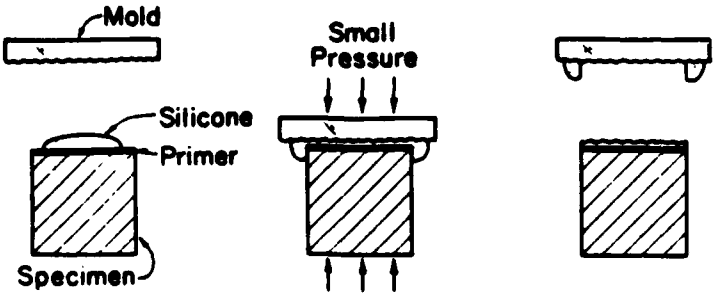

Fig. 2 The crossed-line specimen grating was replicated at 250°F.

$\sin\alpha = f\lambda/2$; $f = 2400$ lines/mm

$U = N_x/f$; $V = N_y/f$

$\epsilon_x = \frac{\partial U}{\partial x}$; $\epsilon_y = \frac{\partial V}{\partial y}$

$\gamma_{xy} = \frac{\partial U}{\partial y} + \frac{\partial V}{\partial x}$

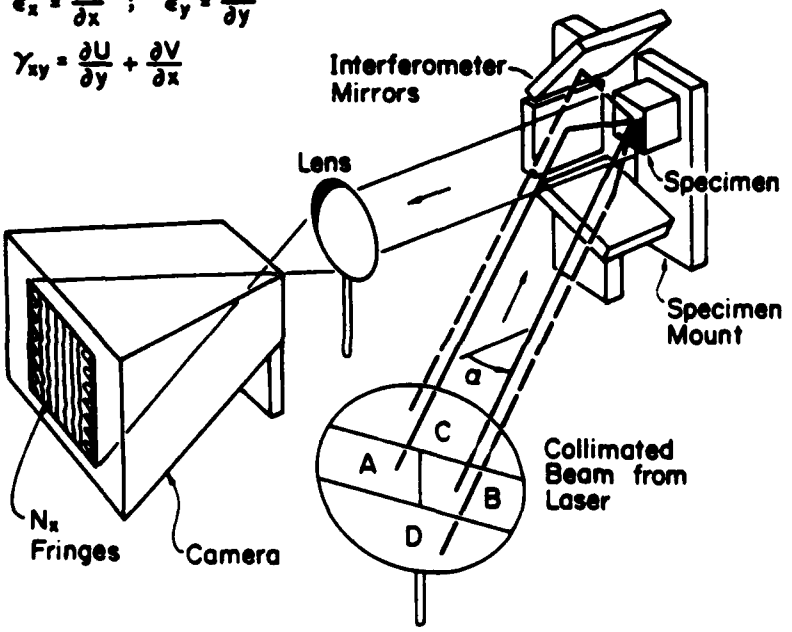

Fig. 3 Apparatus and relationships for moire interferometry.

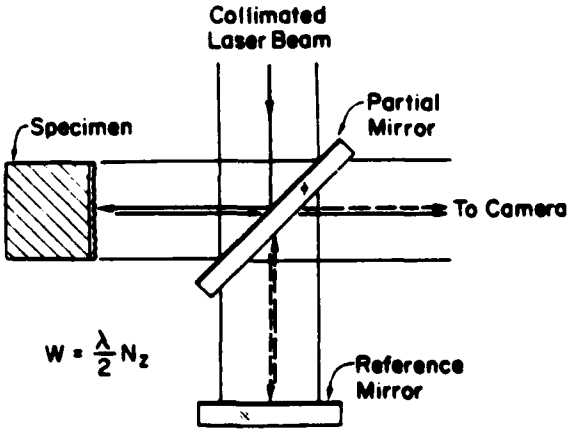

Fig. 4 Twyman-Green interferometer. Light in the zeroth diffraction order of the specimen grating is used.

(a)

(b)

Fig. 5 (a) U displacement field for region in the dashed box.
(b) U field with carrier fringes of extention.

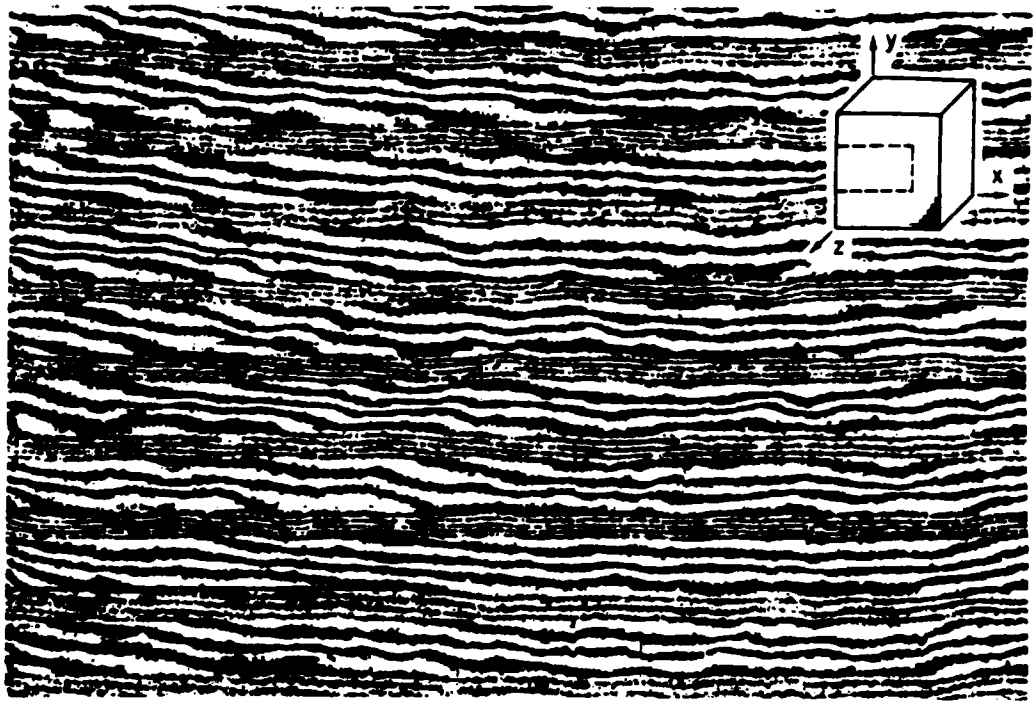

(a)

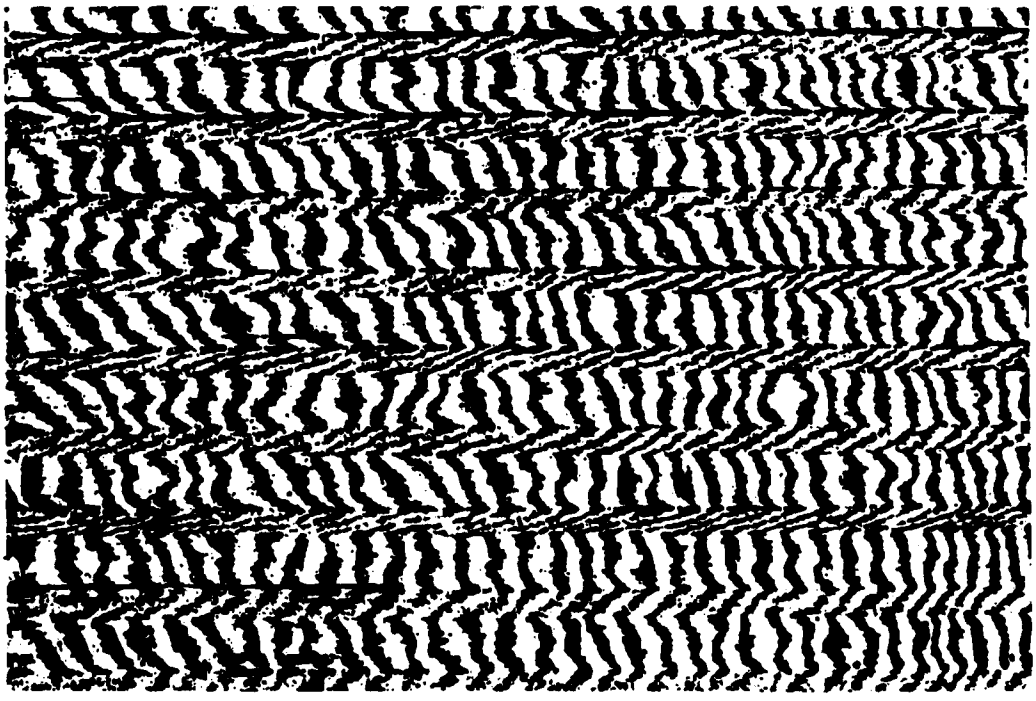

(b)

Fig. 6 (a) V displacement field for region in the dashed box.
(b) V field with carrier fringes of rotation.

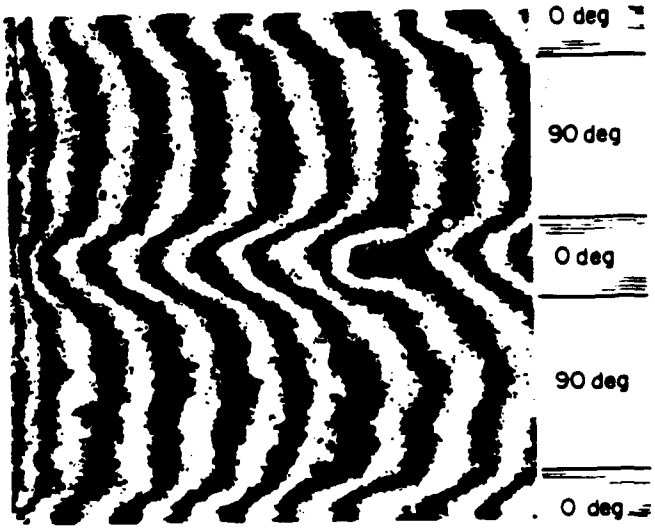

(a)

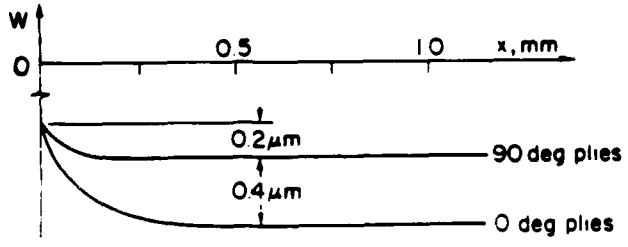

(b)

Fig. 7 (a) Interferogram revealing the surface topography in a local region near the free edge.
(b) Out-of-plane deformations near the free edge of 0 deg and 90 deg plies.

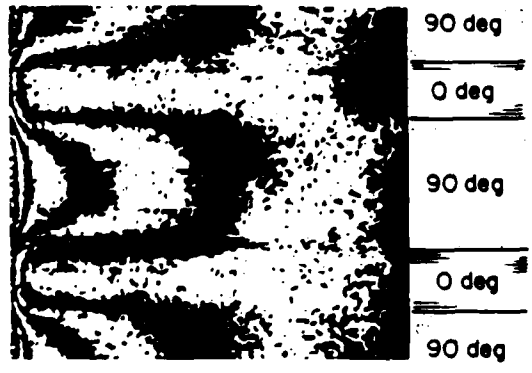

(a)

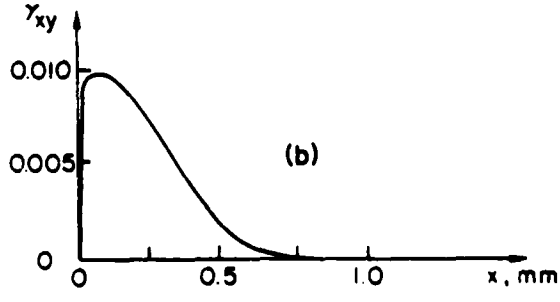

(b)

Fig. 8 (a) U displacement field for local region near the free edge.
(b) Shear strain distribution near the free edge.

END

11-87

DTIC